High Expression of Peroxiredoxin 1 Is Associated with Epithelial-Mesenchymal Transition Marker and Poor Prognosis in Gastric Cancer

Authors' Contribution:
Study Design A
Data Collection B
Statistical Analysis C
Data Interpretation D
Manuscript Preparation E
Literature Search F
Funds Collection G

ACDEFG 1 **Wei Yu**
B 2 **Jing Wu**
B 1 **Zhong-liang Ning**
B 1 **Qiao-yu Liu**
B 1 **Rui-liang Quan**

1 Department of Gastrointestinal Surgery, Anhui Provincial Cancer Hospital, Hefei, Anhui, P.R. China
2 Department of Pathology, Anhui Provincial Cancer Hospital, Hefei, Anhui, P.R. China

Corresponding Author: Wei Yu, e-mail: yuwei025025@163.com
Source of support: Departmental sources

Background: Recent studies show that peroxiredoxin 1 (Prdx1) contributes to the progression and poor prognosis of carcinoma through multiple mechanisms. However, there is little information on its expression and prognostic value in gastric cancer. This study investigated the expression of Prdx1 in gastric cancer, along with evaluating its clinical-pathological and prognostic importance.

Material/Methods: A total of 189 pairs of gastric cancer and paracarcinomatous tissues were assessed for Prdx1 expression and its association with clinical characteristics. The molecular mechanism was further investigated through *in vitro* experimentation.

Results: The mRNA and protein levels of Prdx1 in the GC tissues were higher than in the peri-tumor tissues. We also found that high Prdx1 expression was positively correlated with the lymph node invasion and poor prognosis. It also served as an autonomous prognostic factor for patients with gastric cancer. Moreover, Prdx1 regulates the invasion and metastasis of GC cell lines through inhibiting E-Ca expression.

Conclusions: Prdx1 can promote epithelial-mesenchymal transition and gastric cancer progression. Therefore, it might be a therapeutic target and prognostic indicator for gastric cancer patients.

MeSH Keywords: **Cadherins • Peroxiredoxins • Prognosis • Stomach Neoplasms**

Abbreviations: **Prdx1**– Peroxiredoxin 1; **GC** – gastric cancer; **EMT** – epithelial-mesenchymal transition; **E-Ca** – E-cadherin; **PBS** – phosphate-buffered saline; **DAB** – diaminobenzidine

Full-text PDF: https://www.medscimonit.com/abstract/index/idArt/908722

📄 2546   ▥ 6   📊 7   📰 30

Background

Gastric cancer (GC) is considered the 4th most prevalent malignancy and the 2nd foremost trigger of cancer deaths globally [1]. Accordingly, surgical treatment is the only curative therapeutic option for GC [2,3]. Even though some advances have been made in its retreatment in the recent past, most patients with GC eventually die from recurrence [3]. As such, finding an effective biomarker that can predict the behavior of the tumor is urgently needed in clinical practice.

Peroxiredoxin 1 (Prdx1) is an affiliate of the thiol-dependent peroxiredoxin family of antioxidant enzymes, which regulates the levels of cytokine-induced peroxide. It also facilitates transduction of signal in mammalian cells [4]. Prdx1 activity has previously been reported to be involved in several biological processes, such as differentiation of cells, apoptosis, and proliferation [5]. Many studies have also proposed that Prdx1 can be decontrolled in different cancer types like prostate cancer [6], bladder cancer [7], lung cancer [8], and liver cancer [9].

In the present study, Prdx1 expression was detected and its associations with clinicopathological factors as well as prognosis in GC tissues were examined. Prdx1 was found to be overexpressed in GC tissues at mRNA and protein levels. It was also found to be correlated with a high degree of differentiation and advanced TNM stage. Importantly, Prdx1 overexpression predicted an inferior overall and disease-free survival, and could therefore be a latent self-regulating GC prognostic biomarker. Our study results also suggest that Prdx1 may improve the progression of GC through the mechanism of epithelial-mesenchymal transition (EMT).

Material and Methods

Clinical and tissue samples

Specimens of GC were selected from 189 cases, which were gathered together with the paracarcinomatous tissues, from patients diagnosed at the Anhui Provincial Cancer Hospital (Hefei, China) during the period of 2008 to 2012. From this, comprehensive pathological and clinical data (e.g., age, sex, tumor size, Borrmann type, level of differentiation, histological type, invasion depth, lymph node metastasis, and TNM stage) were acquired from medical records of the patients. The samples were from 134 male and 55 female patients with an average age of 68 years (range: 24–83 years). Tumor stage was then determined as per the 7th edition of the tumor-node-metastasis (TNM) classification of the International Union Against Cancer. None of the patients had undergone radiotherapy or chemotherapy prior to the surgery. Specimens were fixed in formalin, then embedded in paraffin awaiting pathological analysis and diagnosis confirmation. Comprehensive clinical sequel data were obtained from the Anhui Provincial Cancer Hospital GC database. The study was approved by the Human Research Ethics Committee of Anhui Provincial Cancer Hospital, and an informed consent was acquired from every patient.

Immunohistochemistry and scoring

Immunohistochemistry for Prdx1 and E-cadherin (E-Ca) was carried out on every tumor specimen. The tumor samples were cut into sections (4-μm thick) and placed onto silanized glass slides. Then, two-step immunohistochemical was used to detect expression of proteins. In brief, deparaffinized and hydrated sections were preserved with 0.3% hydrogen peroxide in methanol for 15 min at room temperature to obstruct activities of endogenous peroxidase. Then, they were washed in phosphate-buffered saline (PBS; 3×3 min). Antigen retrieval was performed in citrate buffer (pH 6.0). Following washing in PBS (3×3 min), the sections were stained with an Prdx1 monoclonal antibody (Abcam, Cambridge, MA, United States) and E-Ca monoclonal antibody (Beijing Zhongshan Biotechnology, Beijing, China) for about 2 h at 37°C. Then, they were washed in PBS (3 ×3 min). The sections were incubated using the Universal IgG antibody-HRP polymer for about 15 min at 37°C. Subsequently, they were washed 3 times (PBS; 3×3 min). Ultimately, every section was treated using 50 μl diaminobenzidine (DAB) working solution at room temperature for about 3–10 min before washing in PBS. All the sections were counterstained by hematoxylin.

Each of the sections were scored according to the portion of stained tumor cells and the intensity of staining. The proportion of stained tumor cells was categorized as 0 (≤1%), 1 (2% to 25%), 2 (26% to 50%), 2 (51% to 75%), and 4 (≥76%). The intensity of staining was scored as 0 (no staining), 1 (weak), 2 (moderate), and 3 (strong). The outcome of expression was established by use of the following formula: percentage score × intensity score. A general score of 0–12 was considered as low (score: 0–3) or high (score: 4–12). All the stained portions were assessed by 2 pathologists blinded to the data.

Western blotting analysis

Cells were washed in PBS and lysed in RIPA lysis buffer (20 mM HEPES, pH 7.5, 150 mM NaCl, 10% glycerol, 50 mM EDTA, 1% Triton X-100) at 4°C for 30 min. Then, whole-cell extracts were collected and centrifuged at 12 000 rpm for 15 min at 4°C. Afterwards, the supernatants were removed with a pipette and protein concentration was detected using the Bradford method. Equal amounts of lysate protein were resolved by SDS-PAGE and transferred to a nitrocellulose membrane. After that, the membrane was blocked with 5% BSA and incubated in primary antibodies against E-cadherin, Vimentin, Snail,
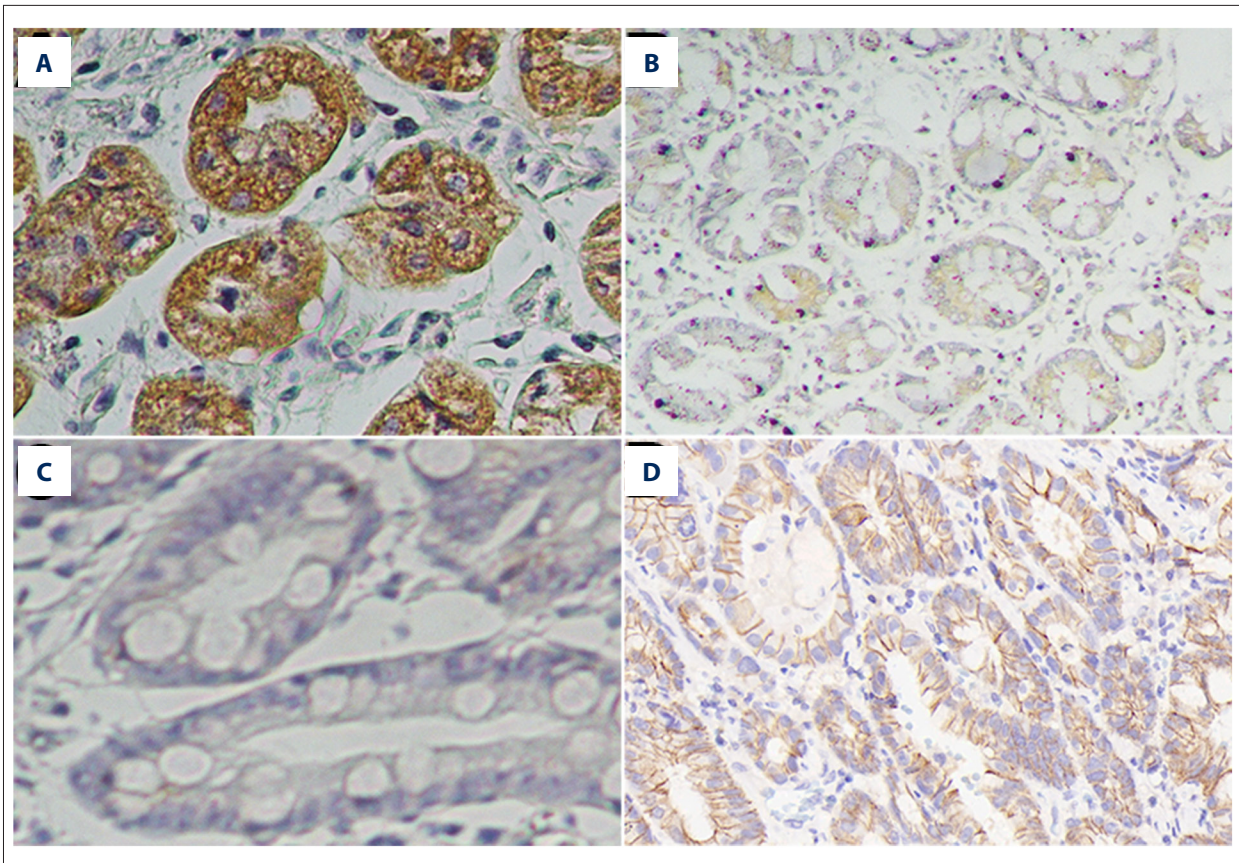
Figure 1. Expression of Prdx1 and E-Ca protein in GC tissue. Immunohistochemistry staining revealed Prdx1 and E-Ca high expression (**A, D**) and low expression (**B, C**).

Prx1, and GAPDH overnight at 4°C. On the next day, the membrane was incubated in a horseradish peroxidase-conjugated secondary antibody and immunoreactive proteins were visualized by an ECL system.

Quantitative real-time PCR

Total RNA was isolated from carcinoma and para-carcinoma tissue treated by TRIzol and DNase I. Total RNA was reverse-transcribed to cDNA by a high-capacity cDNA reverse transcription kit according to the manufacturer's instructions. Snail and Slug mRNA levels were examined by real-time PCR using a SYBR Green quantitative PCR kit (Bio-Rad) and a C1000™ thermal cycler. PCR primer sequences were as follow: human Prdx1, forward 5'-CCACGGAGATCATTGCTTTCA-3' and reverse 5'-AGGTGTATTGACCCATGCTAGAT-3'. Each sample was tested in triplicate and expression of each target was normalized to that of the human GAPDH gene.

Cell culture and treatment

The human Prx1 gene sequence was ascertained in a human placental cDNA library. The human gastric cancer cell line was cultured in DMEM medium supplemented with 10% fetal bovine serum (FBS), penicillin (100 units/mL), and streptomycin (100 lg/mL). The cells were incubated at 37°C and in a humidified environment of 5% CO_2. We used 20 nM siRNA or pC3.1-myc-hPrx1 plasmid in the transfection with Lipofectamine 2000 according with the manufacturer's protocol. Prx1 siRNA (si-Prx1) oligos were as follow: sense 5'-GCCGAAUUGUGGGUGUCUUAUU-3' and antisense 5'-UAAGACACCACAAUUCGGCUU-3'. Cell morphology was observed using an inverted phase-contrast microscope.

Transwell invasion and metastasis experiments

Cells were cultured in 6-well plates at 37°C with 5% CO_2 in 1640 medium with 1% penicillin and streptomycin and 10% FBS until the cells had grown to confluence. Then, the monolayer of cells was wounded with pipette tips, washed with PBS to wipe off the deciduous cells, and incubated for 24 h. The degree of cell migration was determined by the images of the wounded area taken by microscopy (Leica DMi8, Solms, Germany).

Transwell inserts (Corning Costar, Cambridge, MA, USA) were coated with Matrigel Basement Membrane Matrix and incubated for 30 min at 37°C. We pipetted 2×10⁵ cells suspended in
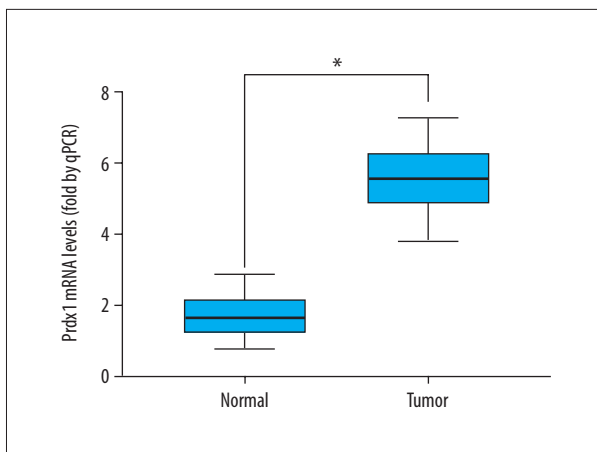
Figure 2. The levels of Prdx1 mRNA in 60 paired GC and corresponding adjacent normal tissues were measured by RT-PCR.
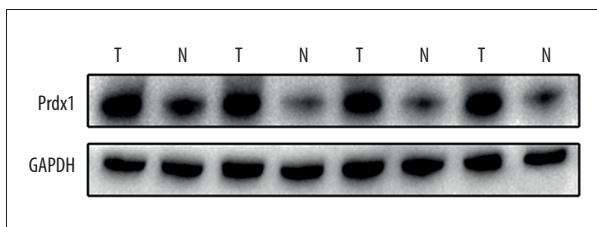

Figure 3. The levels of Prdx1 protein in 4 paired GC and corresponding adjacent normal tissues were measured by Western blotting.

serum-free 1640 medium into the upper chamber and 500 μl 1640 medium with 10% FBS was added in the bottom chambers. After 24-h incubation, the Transwell plates were fixed by paraformaldehyde for 5 min and stained with crystal violet for 1 min. After that, the cells in the upper chamber were eliminated using a cotton swab and invasive cells were photographed using a digital camera (OLYMPUS BX43, Tokyo, Japan).

Statistical analysis

All the statistical evaluations were carried out using the statistical package SPSS 17.0 (SPSS, Inc., Chicago, IL, USA). We used the chi-square test and Spearman correlation test in analyzing

the results of immunohistochemistry. Then, the Kaplan-Meier technique and log-rank test were used in survival analysis. The Cox regression model was used in determining the value of independent prognostic factors. All P values were 2-sided and $P<0.05$ was regarded as statistically significant.

Results

Prdx1 and E-Ca expression in cancerous gastric tissues

In further evaluating the expression level of Prdx1 and E-Ca in GC tissues, we detected the protein expression of Prdx1 and E-Ca in 189 GC tissue samples compared with matched adjacent non-cancerous gastric tissue samples. High and low expressions of Prdx1 and E-Ca in GC tissues are displayed in Figure 1, showing that Prdx1 staining was greatest in the tumor cells' cytoplasm. Consistent with the above observation, the mRNA and protein levels of Prdx1 in the GC tissues were higher than in the corresponding peri-tumor tissues (Figures 2, 3). High expression of Prdx1 was found in most of the GC tissue samples (127/189) but was found in fewer of the non-cancerous gastric tissue samples (43/189). Accordingly, the Prdx1 expression in GC was substantially higher as compared with that of the non-cancerous tissue samples (P<0.001). There was also an observable significant correlation between the expression of Prdx1 and E-Ca, as shown in Table 1. High expression of Prdx1 was associated with low expression of E-Ca (r=–0.154, P=0.035) in GC tissues.

Association of Prdx1 and E-Ca expression with clinicopathological parameters

In examining the functions of Prdx1 and E-Ca in GC tissues, we assessed the relationship of their expressions and the clinicopathological parameters of the GC patients. The expression of Prdx1 was significantly linked to the level of differentiation (P=0.006), invasion depth (P=0.001), lymph node metastasis (P=0.029), and TNM stage (P<0.001), as illustrated in Table 2. In addition, E-Ca expression was higher in early-stage tumors (P=0.037). Statistical analysis showed that expression of E-Ca was correlated with the level of differentiation (P=0.033) and the depth of invasion (P<0.001). The detailed results are shown in Table 2.

Table 1. Expression correlation of Prdx 1 with E-ca in gastric cancer tissues.

Group	Prdx 1 expression		r	P-value
	High	**Low**		
E-Ca expression			−0.154	0.035
High	49	34		
Low	78	28		

Table 2. Relationships between Prdx 1 and E-Ca protein expressions (immunohistochemical staining) in gastric cancer tissues and various clinicopathological variables.

Variables	Total	Prdx 1 expression				E-Ca expression			
		Low (n=62)	High (n=127)	χ^2	P	Low (n=106)	High (n=83)	χ^2	P
Gender									
Male	134	42	92	0.446	0.504	77	57	0.355	0.551
Female	55	20	35			29	26		
Age at surgery (yeas)									
≤60	90	34	56	1.928	0.165	48	42	0.528	0.467
>60	99	28	71			58	41		
Size of primary tumor (cm)									
≤5	95	31	64	0.003	0.959	51	44	0.447	0.504
>5	94	31	63			55	39		
Borrmann type									
I+II type	63	21	42	0.012	0.913	32	31	1.074	0.300
III+IV type	126	41	85			74	52		
Degree of differentiation									
Well/moderate	86	37	49	7.476	0.006*	41	45	4.532	0.033*
Poor and not	103	25	78			65	38		
Histological type									
Adenocarcinoma	160	54	106	0.423	0.515	92	68	0.848	0.357
Others	29	8	21			14	15		
Depth of invasion									
T1	8	5	3	15.592	0.001*	1	7	18.040	0.000*
T2	22	14	8			6	16		
T3	59	18	41			41	18		
T4	100	25	75			58	42		
Lymph node metastasis									
N0	43	19	24	9.060	0.029*	22	21	0.753	0.861
N1	47	20	27			26	21		
N2	54	14	40			31	23		
N3	45	9	36			27	18		
TNM stage									
I	13	9	4	19.911	0.000*	3	10	8.502	0.037*
II	63	29	34			34	29		
III	100	22	78			59	41		
IV	13	2	11			10	3		

Table 3. Univariate analysis of the correlation between clinicopathological parameters and overall survival time of patients with gastric cancer.

Variable	Mean survival time (m)	95% CI	Log-rank test	P
Gender				
Male	45.176	40.777–49.575	0.185	0.667
Female	43.625	36.506–50.743		
Age at surgery(yeas)				
≤60	46.517	41.149–51.886	0.728	0.394
>60	43.265	38.076–48.455		
Size of primary tumor (cm)				
≤5	43.930	38.878–48.983	0.269	0.604
>5	45.856	40.346–51.367		
Borrmann type				
I+II type	46.424	39.813–53.036	0.383	0.536
III+IV type	43.865	39.332–48.398		
Degree of differentiation				
Well/moderate	50.851	45.619–56.084	9.127	0.003
Poor and not	39.423	34.335–44.511		
Histological type				
Adenocarcinoma	43.538	39.499–47.577	2.325	0.127
Others	50.305	41.127–59.483		
Depth of invasion				
T1	71.000	69.303–72.697	26.470	0.000
T2	62.943	54.835–71.051		
T3	44.625	37.253–51.997		
T4	42.050	36.672–47.428		
Lymph node metastasis				
N0	53.041	45.855–60.226	19.629	0.000
N1	53.249	46.494–60.005		
N2	40.014	33.478–46.550		
N3	33.437	25.676–41.198		
TNM stage				
I	71.200	69.798–72.602	58.227	0.000
II	49.310	43.488–55.132		
III	41.753	36.547–46.959		
IV	14.115	10.384–17.846		
Prdx 1 expression				
Low	58.502	53.447–63.556	20.998	0.000
High	38.207	33.658–42.756		
E-Ca expression				
Low	36.536	31.926–41.146	19.155	0.000
High	54.224	48.989–59.458		

Table 4. Multivariate analysis of the correlation between clinicopathological parameters and overall survival time of patients with gastric cancer.

| Covariates	HR	95% CI for HR	P
Gender (Male *vs*. Female)	0.913	0.579–1.439	0.694
Age (≥60 *vs*. <60 cm)	1.080	0.718–1.624	0.713
Tumor size (≥5 *vs*. <5 cm)	0.839	0.548–1.284	0.418
Borrmann type (type I, II *vs*. III, IV)	1.075	0.691–1.672	0.748
Degree of differentiation	0.728	0.475–1.114	0.144
Histological type	1.759	0.920–3.363	0.088
Depth of invasion (T3, T4 *vs*. T1, T2)	0.236	0.088–0.638	0.004
Lymph node metastasis	0.333	0.156–0.711	0.005
TNM stage (stage I *vs*. II *vs*. III *vs*. IV)	1.911	0.851–4.292	0.117
Prdx 1 expression (low *vs*. high)	0.411	0.242–0.700	0.001
E-Ca expression (low *vs*. high)	1.698	1.082–2.664	0.021
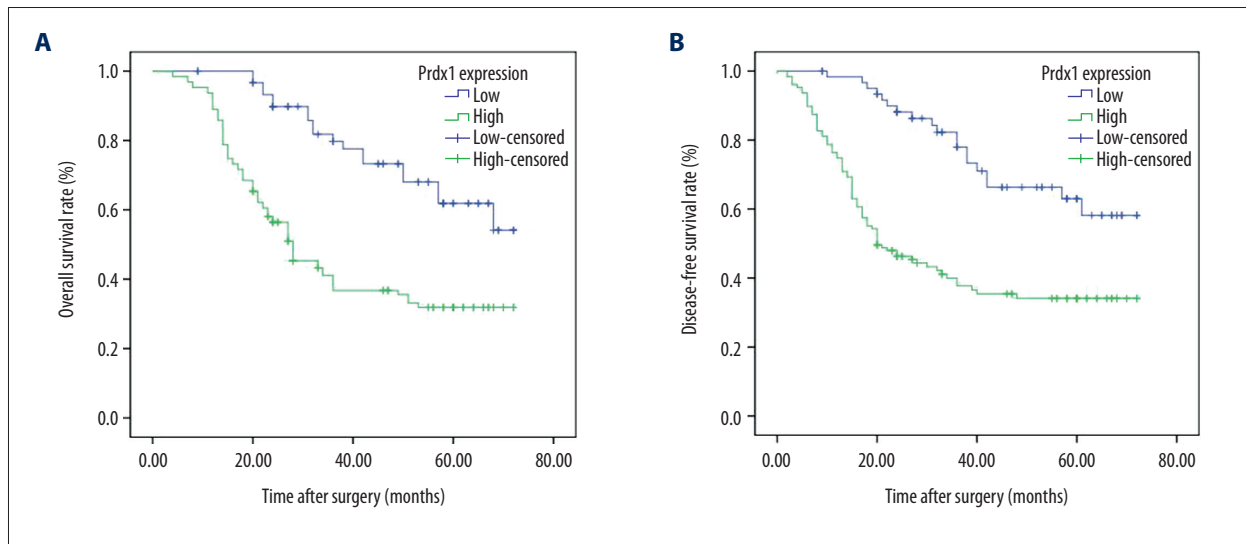
Figure 4. Kaplan-Meier survival curves for OS and DFS according to the high and low expression of Prdx1 from 189 patients with GC. (**A**) Patients with high expression of Prdx1 showed a poor OS (P<0.001). (**B**) Patients with high expression of Prdx1 had a poor DFS (P<0.001).

Correlation of Prdx1 and E-Ca expression with prognosis

The association of Prdx1 expression with prognosis was further analyzed by use of Kaplan-Meier survival curve and log-rank test. The Kaplan-Meier curves were plotted in comparing the OS and the DFS according to the Prdx1 expression patterns. We found that patients who had high expression of Prdx1 had worse OS (38.207 months, P<0.001) and DFS (35.519 months, P<0.001) than in those who had low Prdx1 expression (58.502 months, P<0.001; 56.937 months, P<0.001), as shown in Tables 3, 4 and Figure 4. In contrast, the low expression of

E-Ca was significantly associated with poor OS (P<0.001) and poor DFS (P<0.001) (Figure 5). In the multivariate analysis, depth of invasion (P=0.004 for OS, P=0.006 for DFS), lymph node metastasis (P=0.005 for OS, P=0.006 for DFS), Prdx1 expression (P=0.001 for OS, P=0.001 for DFS), and E-Ca expression (P=0.021 for OS, P=0.013 for DFS) were the independent factors (Tables 5, 6).
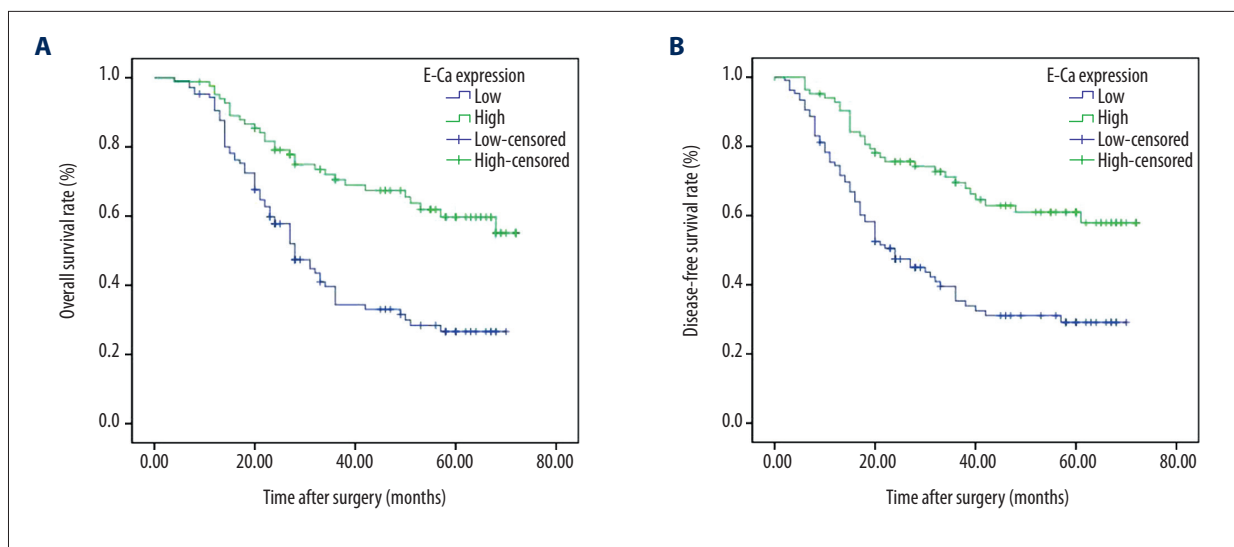
Figure 5. Kaplan-Meier survival curves for OS according to the high and low expression of E-Ca from 189 patients with GC. (**A**) Patients with high expression of E-Ca showed a favorable OS (P<0.001). (**B**) Patients with high expression of E-Ca had a favorable DFS (P<0.001).

Prdx1 promotes GC cell invasion and metastasis through EMT mechanism

To further explore the role of Prdx1 in GC, the GC cell lines (SGC-7901 and MGC-803) were used. As shown in Figure 6, inhibition of Prdx1 significantly attenuated the invasion and metastasis ability of SGC-7901 and MGC-803 cell lines. Additionally, we also detected the EMT-related markers (E-Ca, Snail, and Vimentin) in the GC cells after inducing Prdx1 deficiency. The Western blotting results revealed that the protein levels of these EMT-related markers were significantly downregulated at 48 h after transfection with si-Prdx1 in the GC cells in comparison with the blank control cells (Figure 7).

Discussion

It is well known that gastric cancer is among the foremost causes of cancer-related deaths globally [1]. In assessing prognosis for GC patients, the TNM staging system and the Lauren classification system have been extensively used in clinical practice [10]. Nonetheless, these predictive models are not helpful indicators of prognosis in GC patients. As such, identifying molecules with tumorigenic properties has contributed to the understanding of tumor progression in gastric cancer.

Recent evidence from several publications show that Prdx1 expression patterns are associated with human cancers [11]. Prdx1 facilitates the tumor-suppressive role of PTEN through binding PTEN and shielding its lipid phosphatase activity from H_2O_2-induced inactivation [12]. Additionally, Prdx1 hypermethylation and abridged expressions have been noted

in oligodendroglial tumors. Knockdown of Prdx1 substantially amplifies apoptosis and reduces viability of Hs683 glioma cells subjected to ionizing irradiation or temozolomide *in vitro* [13]. Prdx1 averts ROS-induced senescence in breast cancer by stimulating MKP-5 activity [14].

Many studies have shown that Prdx1 is overexpressed in ESCC cells compared to non-cancerous esophageal epithelial cells [15,16]. In the same way, elevated Prdx1 tends to facilitate tumorigenesis by controlling mTORp70S6K pathway activity in ESCC [16]. Also, Prdx1 is upregulated in NSCLC tissue interstitial fluid, and a high degree of Prdx1 expression may be associated with lymph node metastasis and tumor differentiation, which suggests that Prdx1 is a neoplastic progression marker [17]. Elevated Prdx1 advances prostate tumor vasculature and exhibits upregulation of antigenic proteins, including VEGF, in the tumor region. On the other hand, suppressing of Prdx1 in prostate cancer cell lines tends to reduce formation of tumor vascular, and brings about VEGF downregulation [18,19]. Our study is the first to demonstrate a link between high Prdx1 expression and poor prognosis in GC patients after surgery. Our work demonstrates that Prdx1 plays a role in advancement of GC. Nonetheless, further studies are needed to advance understanding of the molecular mechanism and the latent roles of Prdx1 in GC.

EMT is a central driver of epithelial-derived tumor malignancies. It has been shown to trigger the dissociation of carcinoma cells from primary carcinomas, which subsequently migrate and disseminate to distant sites [20,21]. There has also been a number of confirmed associations between EMT activation and improved tumorigenesis in different human cancer

Table 5. Univariate analysis of the correlation between clinicopathological parameters and disease-free survival time of patients with gastric cancer.

Variable	Mean survival time (m)	95% CI	Log-rank test	P
Gender				
Male	42.675	37.864–47.487	0.026	0.873
Female	41.668	34.077–49.260		
Age at surgery (yeas)				
≤60	44.413	38.562–50.265	0.624	0.430
>60	40.824	35.209–46.439		
Size of primary tumor (cm)				
≤5	41.283	35.785–46.781	0.274	0.601
>5	43.781	37.813–49.748		
Borrmann type				
I+II type	44.407	37.282–51.531	0.469	0.493
III+IV type	41.486	36.547–46.424		
Degree of differentiation				
Well/moderate	48.799	43.077–54.521	7.959	0.005
Poor and not	37.144	31.616–42.671		
Histological type				
Adenocarcinoma	41.130	36.762–45.499	1.961	0.161
Others	47.854	37.543–58.165		
Depth of invasion				
T1	69.250	64.582–73.918	28.117	0.000
T2	62.579	54.201–70.958		
T3	42.457	34.491–50.423		
T4	39.473	33.659–45.287		
Lymph node metastasis				
N0	50.574	42.663–58.485	18.060	0.000
N1	51.080	43.649–58.510		
N2	37.015	29.857–44.173		
N3	31.325	22.864–39.787		
TNM stage				
I	70.429	67.577–73.280	45.520	0.000
II	46.928	40.568–53.289		
III	39.531	33.837–45.225		
IV	10.846	6.640–15.052		
Prdx 1 expression				
Low	56.937	51.396–62.477	21.481	0.000
High	35.519	30.553–40.484		
E-Ca expression				
Low	33.797	28.696–38.898	18.717	0.000
High	52.490	46.853–58.127		

Table 6. Multivariate analysis of the correlation between clinicopathological parameters and disease-free survival time of patients with gastric cancer.

| Covariates	HR	95% CI for HR	P
Gender (Male *vs.* Female)	1.014	0. 645–1.595	0.952
Age (≥60 *vs.* <60 cm)	1.092	0. 726–1. 642	0.673
Tumor size (≥5 *vs.* <5 cm)	0.871	0. 571–1. 329	0.523
Borrmann type (type I, II *vs.* III, IV)	1.030	0. 664–1. 597	0.897
Degree of differentiation	0.761	0. 497–1.165	0.208
Histological type	1.483	0. 879–3.218	0.116
Depth of invasion (T3, T4 *vs.* T1, T2)	0.248	0.092–0.664	0.006
Lymph node metastasis	0.342	0.160–0.733	0.006
TNM stage (stage I *vs.* II *vs.* III *vs.* IV)	1.846	0.825–4.131	0.135
Prdx 1 expression (low *vs.* high)	0.405	0.239–0.687	0.001
E-Ca expression (low *vs.* high)	1.762	1.125–2.762	0.013
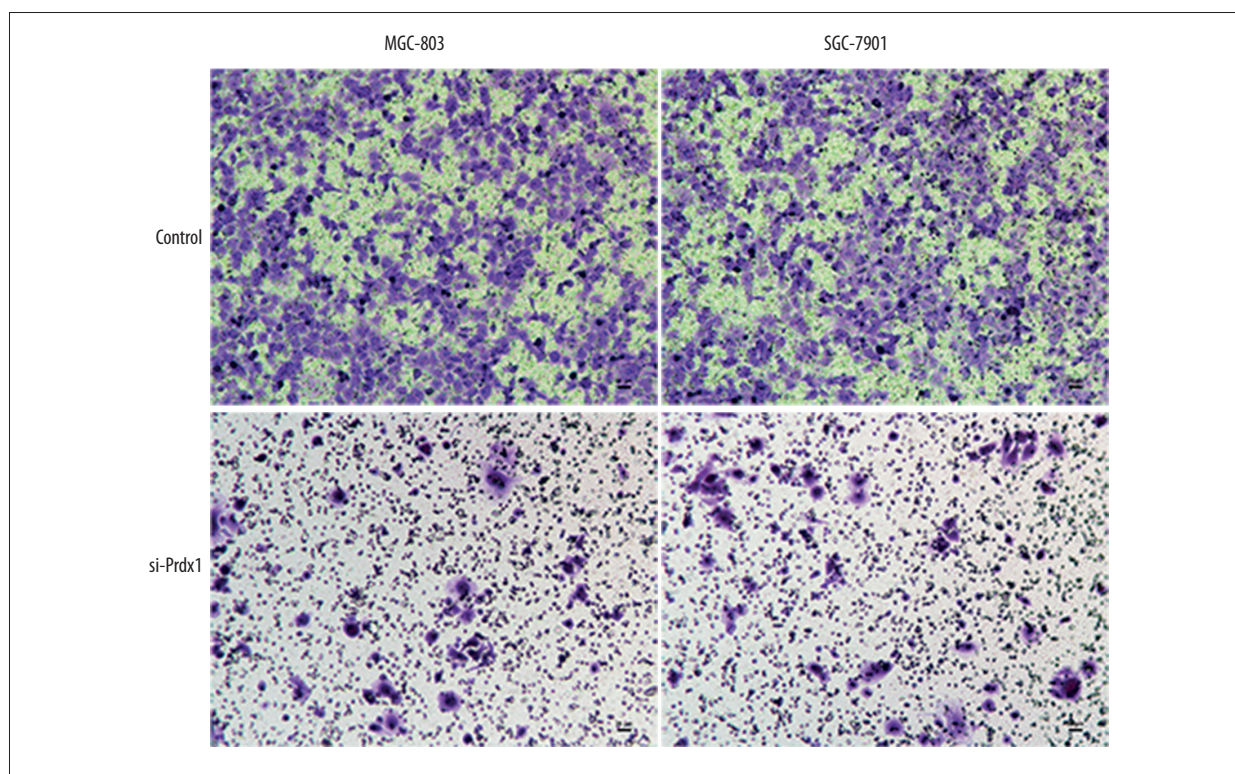
Figure 6. Transwell experiment revealed that the invasion and metastasis ability of GC cell lines was attenuated by inhibiting Prdx1 expression.
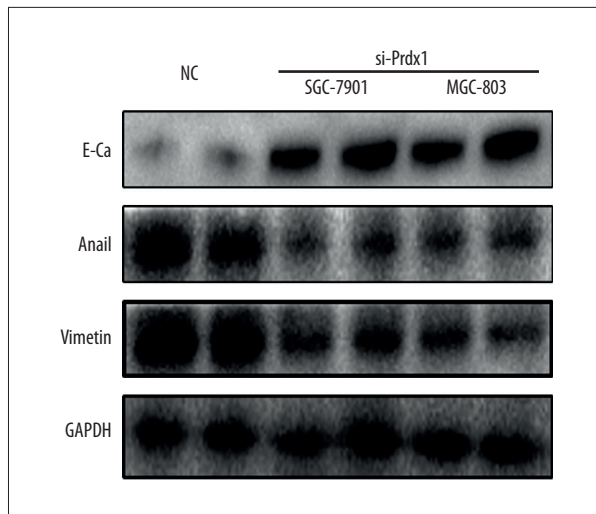
Figure 7. EMT-related markers expression in the GC cells transfected with si-Prdx1 or controls were measured by Western blotting.

cell lines [22]. As such, carcinoma cells with activated EMT program might uphold its continual expression in a cell-independent way by means of self-reinforcing positive-feedback loops [23]. For instance, for breast cancer, achievement of mesenchymal facets is positively correlated with more destructive subtypes of this disease and tumor development [24–26]. Different studies have also demonstrated that EMT participates in the generation, development, and metastasis of GC [27–29]. Emerging evidence shows that human Prdx1 modulates epithelial-mesenchymal transition through its peroxides activity in A549 lung adenocarcinoma cells [30]. The present study

illustrates the association between EMT and Prdx1 in GC and shows high expression of Prdx1 (67.2%) but low expression of E-Ca (56.1%) in gastric cancer tissues. We established a substantial relationship between Prdx1 and EMT based on the expression of Prdx1 and E-Ca. High expression of Prdx1 was found to be related to poor differentiation, deeper invasion, and advanced TNM stage of GC, along with significant association of low expression of E-Ca. High expression of Prdx1 or low expression of E-Ca suggests a poor prognosis. *In vitro* experimentation validated that Prdx1 promotes the invasion and metastasis activity of GC cell through the mechanism of EMT. Taken all together, our findings suggest a connection between Prdx1 and EMT in GC tissues.

One of the main limitations of our single-center study is the relatively small sample size. In addition, the retrospective design may have contributed to selection bias. Accordingly, a prospective study with a larger cohort of patients is needed to confirm our findings. Also, more studies are needed to determine the mechanism by which EMT and Prdx1 interact with each other.

Conclusions

Our study has demonstrated that upregulation of Prdx1 is correlated with progression of tumors in GC. We carried out primary research to explore the relationship between EMT and Prdx1. Further studies on the biological significance of elevated expression of Prdx1 in GC are needed and will help determine if the expression level of Prdx1 can be used as a prognostic biomarker for GC.

References:

1. Torre LA, Siegel RL, Ward EM et al: Global cancer incidence and mortality rates and trends – an update. Cancer Epidemiol Biomarkers Prev, 2016; 25(1): 16–27

2. Van CE, Sagaert X, Topal B et al: Gastric cancer. Lancet, 2016; 388(10060): 2654–64

3. Bertuccio P, Liliane C, Levi F et al: Recent patterns in gastric cancer: A global overview. Int J Cancer, 2009; 125(3): 666–73

4. Hirotsu S, Abe Y, Okada K et al: Crystal structure of a multifunctional 2-Cys peroxiredoxin heme-binding protein 23 kDa/proliferation-associated gene product. Proc Natl Acad Sci USA, 1999; 96(22): 12333–38

5. Jang HH, Lee KO, Chi YH et al: Two enzymes in one; 2 yeast peroxiredoxins display oxidative stress-dependent switching from a peroxidase to a molecular chaperone function. Cell, 2004; 117(5): 625–35

6. Riddell JR, Bshara W, Moser MT et al: Peroxiredoxin 1 controls prostate cancer growth through Toll-like receptor 4-dependent regulation of tumor vasculature. Cancer Res, 2011; 71(5): 1637–46

7. Quan C, Cha EJ, Lee HL et al: Enhanced expression of peroxiredoxin I and VI correlates with development, recurrence and progression of human bladder cancer. J Urol, 2006; 175(4): 1512–16

8. Kim JH, Bogner PN, Baek SH et al: Up-regulation of peroxiredoxin 1 in lung cancer and its implication as a prognostic and therapeutic target. Clin Cancer Res, 2008; 14(8): 2326–33

9. Sun QK, Zhu JY, Wang W et al: Diagnostic and prognostic significance of peroxiredoxin 1 expression in human hepatocellular carcinoma. Med Oncol, 2014; 31(1): 1–9

10. Edge SB, Compton CC: The American Joint Committee on Cancer: The 7th Edition of the AJCC Cancer Staging Manual and the Future of TNM. Ann Surg Oncol, 2010; 17(6): 1471–74

11. Ding C, Fan X, Wu G: Peroxiredoxin 1 – an antioxidant enzyme in cancer. J Cell Mol Med, 2016; 21(1): 193–202

12. Cao J, Schulte J, Knight A et al: Prdx1 inhibits tumorigenesis via regulating PTEN/AKT activity. EMBO J, 2009; 28(10): 1505–17

13. Dittmann LM, Danner A, Gronych J et al: Downregulation of PRDX1 by promoter hypermethylation is frequent in 1p/19q-deleted oligodendroglial tumours and increases radio- and chemosensitivity of Hs683 glioma cells *in vitro*. Oncogene, 2012; 31(29): 3409–18

14. Turnerivey B, Manevich Y, Schulte J et al: Role for Prdx1 as a specific sensor in redox-regulated senescence in breast cancer. Oncogene, 2013; 32(45): 5302–14

15. Gong FH, Liu HT, Li J et al: Peroxiredoxin 1 is involved in disassembly of flagella and cilia. Biochem Biophys Res Commun, 2014; 444(3): 420–26

16. Gong F, Hou G, Liu H et al: Peroxiredoxin 1 promotes tumorigenesis through regulating the activity of mTOR/p70S6K pathway in esophageal squamous cell carcinoma. Med Oncol, 2015; 32(2): 455

17. Li S, Wang R, Zhang M et al: Proteomic analysis of non-small cell lung cancer tissue interstitial fluids. World J Surg Oncol, 2013; 11: 173

18. Riddell JR, Bshara W, Moser MT et al: Peroxiredoxin 1 controls prostate cancer growth through Toll-like receptor 4-dependent regulation of tumor vasculature. Cancer Res, 2011; 71(5): 1637–46

19. Riddell JR, Maier P, Sass SN et al: Peroxiredoxin 1 stimulates endothelial cell expression of VEGF via TLR4 dependent activation of HIF-1α. PLoS One, 2012; 7(11): e50394

20. Cano A, Pérezmoreno MA, Rodrigo L et al: The transcription factor snail controls epithelial-mesenchymal transitions by repressing E-cadherin expression. Nat Cell Biol, 2000; 2(2): 76–83

21. Thiery JP, Acloque H, Huang RY et al: Epithelial-mesenchymal transitions in development and disease. Cell, 2009; 139(5): 871–90

22. Creighton CJ, Chang JC, Rosen JM: Epithelial-mesenchymal transition (EMT) in tumor-initiating cells and its clinical implications in breast cancer. J Mammary Gland Biol Neoplasia, 2010; 15(2): 253–60

23. Scheel C, Eaton EN, Li SH et al: Paracrine and autocrine signals induce and maintain mesenchymal and stem cell states in the breast. Cell, 2011; 145(6): 926–40

24. Aleskandarany MA, Negm OH, Green AR et al: Epithelial mesenchymal transition in early invasive breast cancer: An immunohistochemical and reverse phase protein array study. Breast Cancer Res Treat, 2014; 145(2): 339–48

25. Blanco MJ, Moreno BGD, Locascio A et al: Correlation of Snail expression with histological grade and lymph node status in breast carcinomas. Oncogene, 2002; 21(20): 3241–46

26. Blick T, Widodo E, Hugo H et al: Epithelial mesenchymal transition traits in human breast cancer cell lines. Clin Exp Metastasis, 2008; 25(6): 629–42

27. Liu X, Li Z, Song Y et al: AURKA induces EMT by regulating histone modification through Wnt/β-catenin and PI3K/Akt signaling pathway in gastric cancer. Oncotarget, 2016; 7(22): 33152–64

28. Xie R, Wang X, Qi G et al: DDR1 enhances invasion and metastasis of gastric cancer via epithelial-mesenchymal transition. Tumor Biol, 2016; 37(9): 12049–59

29. Guo W, You X, Xu D et al: PAQR3 enhances Twist1 degradation to suppress epithelial-mesenchymal transition and metastasis of gastric cancer cells. Carcinogenesis, 2016; 37(4): 397–407

30. Ha B, Kim EK, Kim JH et al: Human peroxiredoxin 1 modulates TGF-β1-induced epithelial-mesenchymal transition through its peroxidase activity. Biochem Biophys Res Commun, 2012; 421(1): 33–37